Electron-phonon renormalization of the absorption edge of the cuprous halides

J. Serrano,[1] Ch. Schweitzer,[2] C. T. Lin,[1] K. Reimann,[3] M. Cardona,[1] and D. Fröhlich[2]
[1]*Max-Planck-Institut für Festkörperforschung, Heisenbergstr. 1, D-70569 Stuttgart, Germany*
[2]*Institut für Physik, Universität Dortmund, D-44221 Dortmund, Germany*
[3]*Max-Born-Institut für Nichtlineare Optik und Kurzzeitspektroskopie, D-12489 Berlin, Germany*
(Received 24 September 2001; published 13 March 2002)

We report the isotope effects of copper and bromine on the gap of CuBr, and that of copper on the gap of CuI. The measured isotope effects reveal an anomalous negative shift with increasing copper mass for the three halides. These results allow us to understand the anomalous temperature dependences of the band gap E_0 in the copper halides, which we report in the case of CuI. Similarities to the behavior observed for the copper and silver chalcopyrites are also pointed out.

DOI: 10.1103/PhysRevB.65.125110 PACS number(s): 71.35.Cc, 71.36.+c, 63.20.Kr

I. INTRODUCTION

The electronic band structure of the cuprous halides differs considerably from that of other tetrahedral semiconductors which contain neither copper nor silver as a cation. It was early recognized that the differences are due to a strong admixture of the $3d^{10}$ copper electrons ($4d^{10}$ in the case of silver) to the conventional, valence-band-forming p electrons of the anion ($2p^7$ for chlorine). Instead of the conventional eight valence electrons of the primitive cell of zinc blende (s^2+p^6) a total of 18 ($d^{10}+s^2+p^6$) hybridized electron states constitute the valence bands of the cuprous halides. The ten d electron states split in the cubic field into six Γ_{15} and four Γ_{12} states. The former hybridize strongly with the six p-like valence states of the halogen atoms, whereas the Γ_{12} states do not hybridize at $\mathbf{k}=0$, but they hybridize with s and p states at a general point of the Brillouin zone (BZ) (continuity requires this hybridization to remain small). This hybridization leads to a number of anomalies, several of them have been discovered after the original suggestion in Ref. 1 (for an early review, see Ref. 2). Among them, we first mention that the lowest gap of these materials (which is direct and occurs at the Γ point, as in GaAs and ZnSe) is lower than expected from extrapolation of their isoelectronic group IV, III-V, and II-VI counterparts (Ge: 0.9 eV; GaAs: 1.5 eV; ZnSe: 2.7 eV; CuBr: 3.0 eV). Even more striking is the fact that the spin-orbit splitting Δ_0 of the uppermost valence band (Γ_{15} splits into Γ_8 and Γ_7 double group representations) is rather small, even negative (Γ_7 above Γ_8) for CuCl.[1,3] Additionally, anomalously small temperature[1] and pressure[4–6] dependences of the gap have also been observed.

The temperature dependence of semiconductor gaps is intrinsically connected to their dependence on isotopic mass. The reason for this is that the temperature dependence is caused, to a large part, by the renormalization of the band gap due to electron-phonon interaction. Because of the zero-point vibrations there is already an effect at zero temperature, which is proportional to the square of the vibrational amplitudes, obviously mass dependent.

During the past ten years a number of experiments[7–12] has been performed on the dependence of the gap on isotopic mass. In compound semiconductors, such experiments yield considerably more information than temperature-dependent experiments, since the mass of each constituent element can have a different effect on a given gap.[7,12] Of particular interest is the case of CuCl: an increase of the chlorine mass (from ^{35}Cl to ^{37}Cl) leads to the usual increase of the E_0 gap, whereas the increase of the copper mass (from ^{63}Cu to ^{65}Cu) results in an anomalous decrease of the gap.[7] This led to the understanding of the anomalous temperature dependence of the E_0 gap of CuCl reported in Refs. 13–16. Using the same model and the observed data for $E_0(T)$ in CuBr, the authors of Ref. 7 predicted the dependences of the E_0 gap on copper (M_{Cu}) and on bromine mass (M_{Br}).

In this paper we report measurements of $\partial E_0/\partial M_{\mathrm{Cu}}$ and $\partial E_0/\partial M_{\mathrm{Br}}$ for CuBr, which confirm the above conjecture. We also report measurements of $\partial E_0/\partial M_{\mathrm{Cu}}$ for the E_0 gap[17] of CuI. For CuI we also present rather unusual results on the temperature dependence of the E_0 gap. A detailed analysis of electron-phonon renormalization effects is presented which accounts for the weak but considerably structured temperature dependence of the gap. In the temperature range from 0 to 300 K the E_0 gap decreases by 8 meV, in agreement with the early data of Ref. 1. A fit to the experimental $E_0(T)$ data with a three-oscillator model yields values for $\partial E_0/\partial M_{\mathrm{I}}$ and for $\partial E_0/\partial M_{\mathrm{Cu}}$, the latter in good agreement with the directly measured one. The results we obtained for the cuprous halides are used to interpret the anomalies reported for the temperature dependence of the lowest band gap in other tetrahedral compounds like cuprous and silver chalcopyrites,[18–25] which exhibit a small positive slope at low temperatures followed by a sign reversal in the slope above ≈ 100 K.

This paper is organized as follows: We discuss in the next section the peculiar band structure of the cuprous halides in the region around the E_0 gap. Section III contains details about the experimental method. In Sec. IV we present our data for the isotopic dependence of E_0 at low temperature for CuI and CuBr and for the temperature dependence of E_0 for CuI. Then we introduce in Sec. V a model for both temperature and isotope effects and compare our present results with those obtained in Ref. 7 for CuCl. Finally, in Sec. VI, an exhaustive compilation of the anomalies reported in the behavior of the temperature dependence of E_0 is performed for the cuprous and silver chalcopyrites and quantitatively interpreted in terms of our results for the simpler cuprous halides.

II. ELECTRONIC BAND STRUCTURE

The lowest absorption edge (equivalently referred to as lowest gap or lowest exciton) of CuCl differs considerably from that of CuBr and CuI. The difference is due to the anomalous sign of the spin-orbit splitting, which is negative for CuCl, but positive for the other cuprous halides,[1,3,7] a consequence of the negative contribution of the copper $3d$ electrons to the spin-orbit splitting.[3] Hence the symmetry of the uppermost valence band of CuBr and CuI (E_0) is Γ_8, whereas that of CuCl is Γ_7 ($E_0+\Delta_0$). The symmetry of the lowest conduction band is Γ_6 in all cases.

Because of Coulomb interaction, electrons in the conduction band and holes in the valence band form exciton states. Excitons corresponding to the Γ_8 valence band are often labeled $Z_{1,2}$, where Z stands for zinc blende, whereas excitons belonging to the Γ_7 valence band are labeled Z_3. The exciton symmetry is given by the direct product of conduction- and valence-band symmetries. Thus $Z_{1,2}$ excitons ($\Gamma_8\times\Gamma_6$) are eightfold degenerate and split through exchange interaction into Γ_3, Γ_4, and Γ_5 components,[26] whereas the Z_3 fourfold degenerate excitons ($\Gamma_7\times\Gamma_6$), split into Γ_2 and Γ_5. Only the Γ_5 components are dipole allowed and contribute to one-photon absorption processes. Two-photon transitions, on the other hand, are allowed for Γ_1, Γ_3, Γ_4, and Γ_5 excitons. Each of the Γ_5 excitons constitutes a triplet, whose transverse components interact strongly with photons, thus giving rise to exciton-photon coupled states (polaritons).

III. EXPERIMENT

We have performed measurements on samples of CuI and CuBr with all possible combinations of stable isotopes (^{63}Cu, ^{65}Cu; ^{127}I; ^{79}Br, ^{81}Br) and the corresponding natural compositions. Details of the crystal growth have been published elsewhere.[27–29]

To be able to accurately determine the rather small isotope shifts, we have used the nonlinear optical technique of two-photon absorption[30] (TPA), since this technique yields much smaller linewidths than linear optical methods, as, e.g., reflection or absorption (as an example, for CuCl one can compare the absorption data in Ref. 1 with the two-photon data in Refs. 7 and 31). For the same reason we have restricted our measurements to the excitons with the lowest energies, i.e., to the $Z_{1,2}$ excitons in CuBr and CuI, since excitons with higher energies are broadened through phonon-induced decay into lower-energy states.

The classical method[31] for the measurement of TPA is to detect a change in the intensity of the transmitted light of the first beam during the presence of the second (high-intensity) beam. This method is, however, not sensitive enough to detect TPA in our thin samples. Therefore in our case TPA is detected by monitoring the luminescence intensity from a defect-related level below the band gap as a function of the sum of the two photon energies (the two-photon energy). Since we use two photons from the same laser, the two-photon energy is equal to twice the laser photon energy.

The experimental setup for these measurements consists of an exciting laser, a cryostat with the sample, and the detection system.

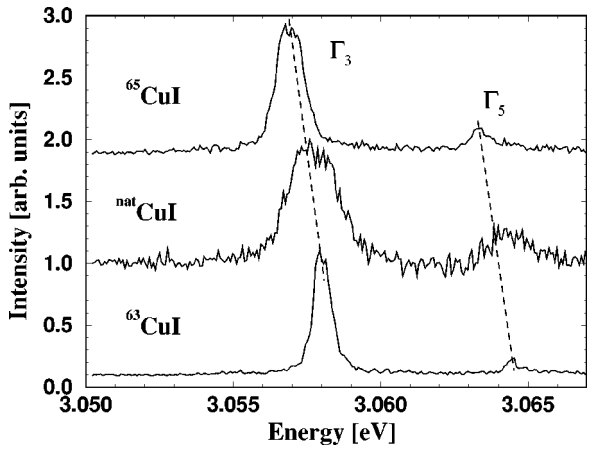

FIG. 1. Two-photon-absorption spectra of isotopically modified CuI measured at 7 K. The two features observed in each spectrum correspond to the Γ_3 and the Γ_5 excitons. The dashed lines are guides to the eye. Note the anomalous negative shift in the peak energies with increasing copper mass.

Since nonresonant in the intermediate state (the photon energies are far from resonances in our experiments) two-photon absorption in these compounds is a very weak effect; high excitation intensities of about 10 MW/cm^2 must be used. They are generated by a Nd:YAG-laser-pumped tunable dye (styril) laser with a pulse width of 5 ns and a repetition rate of 10 Hz.

The samples were mounted strain free in a helium flow cryostat. The temperature, which is measured with a calibrated silicon diode mounted near the samples, can be varied by changing the rate of helium flow and by additional heating. For the measurements of the isotopic effect on the band gap the samples were held at a temperature of 7 K.

The detection system consists of a $f/1.8$ collection optics, a prism spectrometer and appropriate optical filters to separate the weak luminescence from the intense laser light, and a bialkali photomultiplier. The wavelength of the spectrometer is held fixed at the luminescence maximum. The output signal from the photomultiplier is fed into a gated integrator and sent via an analog-digital converter to a personal computer, which also controls the scanning of the dye laser.

IV. RESULTS

A. CuI

Two-photon absorption spectra for CuI with different copper isotopic compositions are shown in Fig. 1. The lower and higher energy peaks we observe are identified as the Γ_3 (with possible admixture of Γ_5 transverse) and Γ_5 longitudinal excitons.[26,32] The splitting of 6.7 meV between the peaks is in agreement with previously reported values[32] (6.5 meV). Shown in Fig. 2 are the peak energies obtained from a Lorentzian fit vs the average isotopic mass. The values of $\partial E_0/\partial M_{\mathrm{Cu}}$ from a linear least-squares fit are listed in Table I. Although the error bars of the Γ_3 data, -550 ± 12 μeV/amu, are much smaller than those of the weaker Γ_5 data, -510 ± 150 μeV/amu, the agreement between both sets of data is excellent.

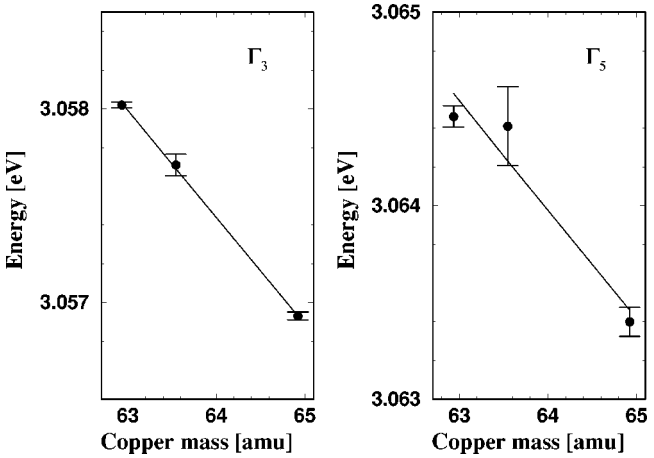

FIG. 2. Isotope mass dependence of the Γ_3 and Γ_5 excitons in CuI. The lines represent least-squares fits to the experimental data from Fig. 1.

Figure 3 shows the measured temperature dependence of the lower-frequency peak of Fig. 1 for natural CuI for temperatures up to 300 K. Measurements at higher temperature are not meaningful because of the increasing linewidth (see error bars in Fig. 3). One should note the following important points: (i) The overall effect of temperature is a decrease in energy, opposite to the observations[7] for CuCl and CuBr. (ii) At about 150 K a change in the slope of $E_0(T)$ is seen, remindful of the behavior observed for CuCl and CuBr. (iii) Below 60 K a weak sigmoidal behavior is observed, with maxima at $T=0$ and $T=40$ K (see inset in Fig. 3).

B. CuBr

Some two-photon spectra for CuBr samples of different isotopic compositions measured at 7 K are displayed in Fig. 4. In contrast to CuI here one observes only the Γ_5 longitudinal exciton. Attempts to observe the Γ_3 exciton revealed that it is at least two orders of magnitude weaker than in CuI. This may be related to the near degeneracy of the Γ_3 and Γ_5 excitons in CuI, which does not occur[32,33] in CuBr. By means of Lorentzian fits we obtain the E_0 energies plotted in Fig. 5 as a function of the corresponding isotopic masses of copper and bromine. Least-squares fits to these points result in the corresponding slopes listed in Table I. The data allow us to establish the anomalous negative sign of the copper mass derivative which was predicted in Ref. 7. Note, however, that in Fig. 4 the E_0 peak of $^{nat}Cu^{nat}Br$ deviates considerably from the dashed line. It is difficult to attribute this deviation to the isotopic disorder of the copper sublattice, which should only produce a broadening of about 0.02 meV, estimated on the same basis as in Ref. 34 for silicon. One may conjecture that because of the small exciton radius of CuBr ($r_{ex}\simeq 12$ Å) the E_0 peak of Fig. 4 for $^{nat}Cu^{nat}Br$ corresponds

TABLE I. Dependence of the exciton energies on isotope mass and corresponding unrenormalized gaps. The values obtained by varying the isotopes of copper and halogen (X) are compared with those found from two-oscillator fits to the temperature dependence, the latter labeled T, L, or M according to the frequencies chosen for each oscillator, i.e., either TA and TO, or LA and LO, or a mixture of tranverse and longitudinal phonons of frequencies in the one-third to two-thirds ratio, respectively. In the case of CuI, a three-oscillator model was necessary to fit the experimental data; we used the average frequencies of the TA, LA, and LO bands. The frequencies are given in K, whereas the derivatives are displayed in μeV/amu. E_0 is given in meV.

Isotope measurements					Temperature data						
					E_0	$\frac{\partial E_0^T}{\partial M_{Cu}}$	$\frac{\partial E_0^T}{\partial M_X}$				
CuX	$\frac{\partial E_0^{\Gamma_3}}{\partial M_{Cu}}$	$\frac{\partial E_0^{\Gamma_3}}{\partial M_X}$	$\frac{\partial E_0^{\Gamma_5}}{\partial M_{Cu}}$	$\frac{\partial E_0^{\Gamma_5}}{\partial M_X}$	E_0	$\frac{\partial E_0^L}{\partial M_{Cu}}$	$\frac{\partial E_0^L}{\partial M_X}$	ω_{TA}	ω_{LA}	ω_{TO}	ω_{LO}
					E_0	$\frac{\partial E_0^M}{\partial M_{Cu}}$	$\frac{\partial E_0^M}{\partial M_X}$				
					3236	-69	546				
CuCl	-81[a]	346[a]	-71	382	3260	-446	1482	51	169	300	333
					3244	-152	773				
					2975	-44	87				
CuBr			-115(90)	132(40)	2984	-378	401	53	158	216	233
					2978	-98	142				
CuI	-550(12)		-510(150)		3045	-524	243	60	156	192	224

[a]Because of the different band-edge structure of CuCl, these data do not correspond to a Γ_3 exciton but to the upper polariton. See Fig. 1 of Ref. 7.

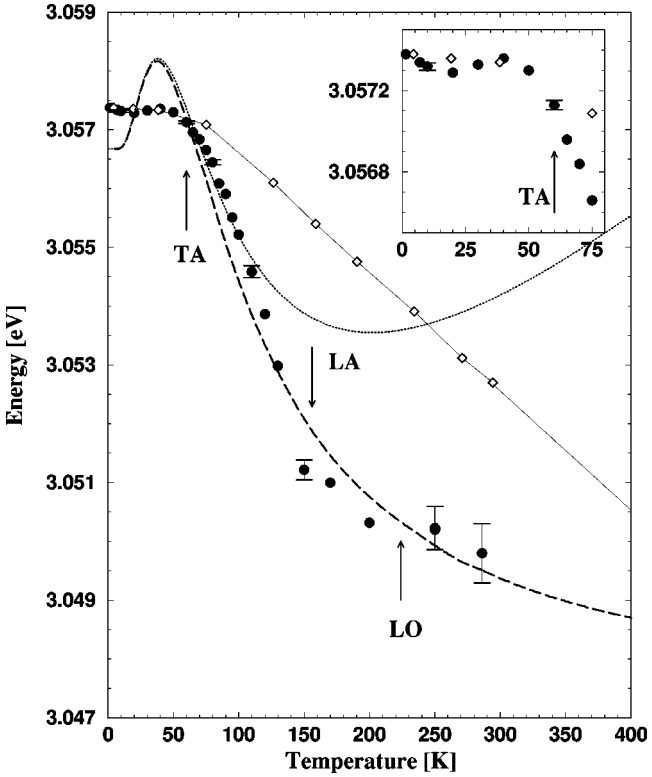

FIG. 3. Temperature dependence of the lowest exciton peak for CuI (equivalent to that of the E_0 gap). The dotted line represents a three-oscillator fit of the difference between the experimental data (solid circles) and the contribution due to the thermal expansion (open diamonds), which is displayed shifted by $E_0(T=0)$ in order to show more clearly the relevance of this term. The dashed line is obtained by adding both contributions. The arrows indicate the frequencies of the three oscillators used in the fit (also listed in Table I). A small sigmoidal dependence is observed at low temperatures (see inset). Note the flattening of the temperature dependence at ≈ 180 K.

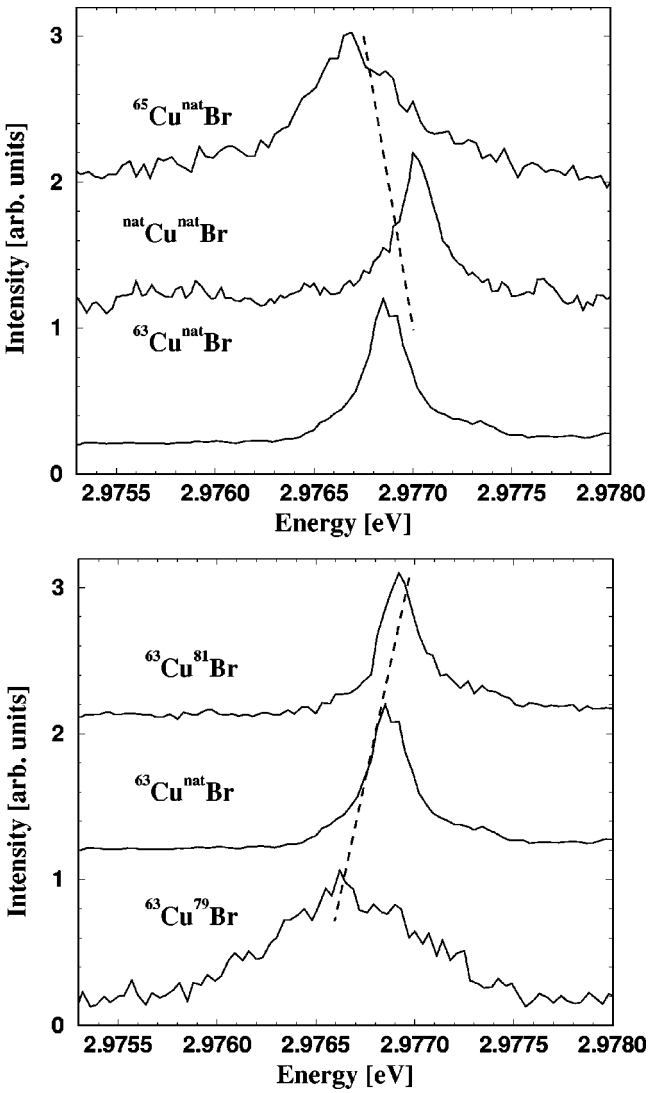

FIG. 4. Two-photon-absorption spectra of CuBr for several isotopic compositions measured at 7 K. The dashed lines are guides to the eye. An anomalous decrease of the exciton energy is observed with increasing copper mass (upper figure), whereas the lower figure displays the usual positive slope with increasing bromine mass.

to clusters of ^{65}Cu^{nat}Br of a size equal to that of the E_0 exciton. Another possible cause is the higher chemical purity of ^{nat}Cu as compared to that used in the preparation of the isotopic samples. We should also keep in mind that the shifts of Figs. 4 and 5 are one-third of those shown in Figs. 1 and 2 for CuI. This may explain why this anomaly is not seen in CuI.

V. DISCUSSION

We assume here, as it was done in previous[1,7] works, that shifts with either temperature or isotopic mass observed for the $Z_{1,2}$ excitons (or for Z_3 in the case of CuCl) are representative of the corresponding one-electron gaps. This assumption is usually justified by the fact that the exciton binding energies, which are very large in the copper halides, are nevertheless more than one order of magnitude smaller than the corresponding band gap. Additionally, one has to consider that for CuCl (and to a lesser extent also for CuBr) the exciton binding energy[35] (≈ 190 meV for CuCl, ≈ 140 meV for CuBr) is close to or larger than another important characteristic energy, that of the spin-orbit splitting Δ_0 (≈ -70 meV for CuCl, ≈ 150 meV for CuBr). Consequently the spin-orbit splitting measured for the exciton should be somewhat smaller than the splitting Δ_0 of the valence bands at the Γ point of the BZ. This decrease in Δ_0, which has been investigated for diamond,[36,37] has not been discussed for CuCl and CuBr. It is nevertheless unlikely that changes in Δ_0 induced by changes either of temperature or of mass will alter our conclusions. This has been confirmed for the temperature dependence[16] of E_0 and $E_0+\Delta_0$ in CuBr (see Fig. 8 of Ref. 7). In any case, for CuI the problem does not arise since[1] $\Delta_0 \approx 630$ meV is much larger than the exciton binding energy[38] (≈ 58 meV).

The model we use here for the description of the mass and temperature dependences of the band gap is the same as in Ref. 7. The effects of both temperature and mass changes can be divided into the effect of the change of lattice constant

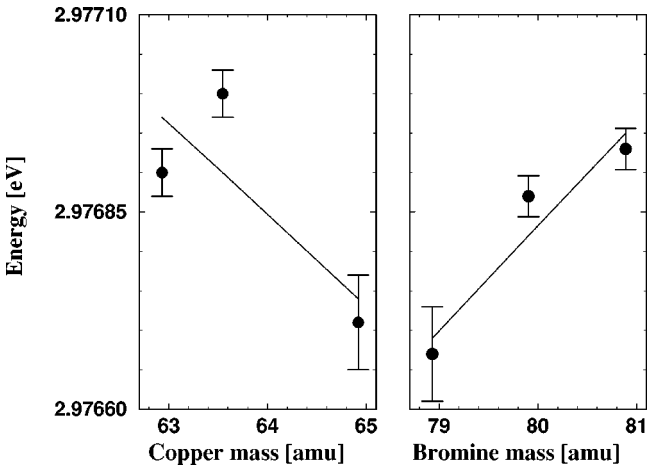

FIG. 5. Dependence of the low-temperature exciton energy in CuBr on copper and bromine masses. The solid lines represent least-squares fits to the data of Fig. 4.

and the renormalization by the electron-phonon interaction. The change in lattice constant leads to the following change of the gap:

$$\Delta_{\text{th}}E_0(X)=3\alpha\frac{a(X)-a_0}{a_0}, \tag{1}$$

with $\alpha=dE_0/d\ln V$ the deformation potential of the E_0 gap and $a(X)$ the lattice constant as a function of X (either temperature or one of the isotopic masses).

In principle, for the calculation of the renormalization by electron-phonon interaction it is necessary to include every possible phonon mode. It turns out, however, that a much simplified model is sufficient for a good description of the data. Instead of using the complete phonon dispersion, we use only two (three for CuI) average phonons. This leads to the following expression:

$$\Delta E(T)=\sum_i \frac{A_i}{\Omega_i M_i}\left[2n_B\left(\frac{\Omega_i}{T}\right)+1\right]. \tag{2}$$

The sum is over the oscillators used, A_i is the electron-phonon coupling coefficient for the oscillator i, Ω_i its frequency (in K), and n_B the corresponding Bose-Einstein factor. M_i is the reduced mass for the vibration considered.

Two oscillators with opposite values of A are required to describe the change in $E_0(T)$ observed at ≈ 100 K for both CuCl and CuBr. The anomalous positive slope for $T<100$ K is due to the copper vibrations ($A_{\text{Cu}}>0$), whereas the decrease in slope for $T>100$ K is due to the vibrations of the halogen, which have negative values of A.

Since it is not clear *a priori* which phonons contribute most to the electron-phonon interaction, i.e., which are the magnitudes and signs of A_i for the various groups of phonons, we compare in Table I different possibilities. We show in this table the experimental results for the isotope dependence together with theoretical values obtained from a two-oscillator fit of the temperature dependence. The three values given in Table I for CuCl and CuBr are obtained by choosing for the two oscillators (T) the average TO and the average TA phonon energy, (L) the LO and the LA phonon energy, or (M) the average of all acoustic-phonon energies and the average of all optical phonon energies, respectively. As one can see, the best agreement between measured and calculated values is reached for CuCl for case T (the same energies were also used in Ref. 7) and for CuBr for case M. At this point we should note that in Ref. 7 copper, in spite of its slightly lighter mass, seemed to play the main role in the acoustic vibrations, whereas bromine was responsible for the optical modes. This *ad hoc* assumption has recently been validated by Raman measurements[27] on isotopically tailored CuBr. A similar assumption is also necessary to explain the present measurements.

In order to get an appropriate description of the temperature dependence of the gap of CuI shown in Fig. 3, the use of a three-oscillator model is necessary. For the frequencies we choose the average TA, LA, and LO phonon energies. The results of this fit, together with the effect of thermal expansion, are shown by the dashed line in Fig. 3. Apart from an overestimate of the amplitude of the low-temperature wiggle, the fit agrees well with the experimental data. Using the model, we obtain a copper isotopic shift of -524 μeV/amu, which agrees perfectly with the measured values (-550 and -510 μeV/amu).

One should note that in CuI the contribution to $E_0(T)$ due to thermal expansion,[39] which is shown by the diamonds in Fig. 3, is very important (it accounts for about two-thirds of the total band gap change). This is in marked contrast to CuCl and CuBr, for which the effect of the thermal expansion is negligible. As mentioned in Ref. 7 the shift between 0 and 300 K for CuBr amounts to 32 meV, the thermal expansion contribution being only 0.7 meV. This small thermal expansion shift is due to the very small value of the gap deformation potential[35] $\alpha=-0.17$ eV defined in Eq. (1). As discussed below, this shift is an order of magnitude larger for CuI (see Fig. 3) because of the much larger[39] (-1.1 eV from Ref. 35) value of α. In the case of CuCl, the relative contribution of the thermal expansion is even smaller (-0.5 meV from a total shift of 50 meV, using $\alpha=-0.35$ eV from Ref. 35).

Figure 3 indicates that the net effect of the electron-phonon interaction (dotted line in Fig. 3) is very small ($\leqslant 5$ meV). This suggests that there is near total compensation between the effects of the copper and the iodine vibrations. The residual effects contain detailed structure, which requires three oscillators for its description. We have placed these three oscillators at the average TA frequency (60 K), LA frequency (156 K), and LO frequency (224 K). An additional oscillator (e.g., at the TO frequency) does not improve the quality of the fit. As adjustable parameters we use the corresponding three coefficients $A_i/(\Omega_i M_i)$ of Eq. (2). In this manner we obtain, after adding the thermal expansion effect, the dashed line of Fig. 3. The coefficient $A_i/\Omega_i M_i$ that corresponds to the TA phonons is found to be about one-tenth of that of the other two phonons. Because of the heavier mass of iodine, the LA coefficient should be proportional to $\partial E_0/\partial M_{\text{I}}$, according to Eq. (2), whereas the LO coefficient should correspond to $\partial E_0/\partial M_{\text{Cu}}$, neglecting the TA coefficient. The corresponding values of $\partial E_0/\partial M_{\text{Cu}}$ and

TABLE II. Temperature shift of the lower absorption gap E_0 for cuprous and silver chalcopyrites. The data are compared with that of the corresponding isoelectronic binary compounds, the cuprous halides, and other binary compounds with zinc-blende crystal structure. T_a stands for the temperature at which a kink is observed in the temperature dependence, and the hydrostatic deformation potential is listed under α. E_0 and $E_0(300\ \mathrm{K})-E_0(0)$ are given in meV, α in eV, and T_a in K.

	$E_0(T=0)$	$E_0(300\ \mathrm{K})-E_0(0)$	T_a	α
$CuAlS_2$ [a]	3510	-45	140	
$CuGaS_2$ [b]	2510	-60	120	
$CuGaSe_2$ [b]	1720	-35	140	-3.9 [c]
$CuGaTe_2$ [d]	1444	-88		-4.6 [c]
$CuInS_2$ [b]	1534	-13	120	
$CuInSe_2$ [b]	990	-23	100	-2.2 [c]
$CuInTe_2$ [e]	1000	-43	200	-3.4 [c]
$AgGaS_2$ [f]	2710	-33	110	
$AgGaSe_2$ [f]	1820	-22	170	-3.2 [c]
$AgInSe_2$ [g]	1200	+10	120	-1.7 [c]
$AgInTe_2$ [h]	1000	-36		
CuCl [i]	3206	+50	100	-0.4
CuBr [i]	2967	+32	100	-0.3
CuI [i]	3057	-8	180	-1.1
AgI [i]	2900	-12		
GaAs [i]	1540	-95		-9.8
GaSb [i]	813	-88		-7.0
ZnSe [i]	2770	-90		-4.9
ZnTe [i]	2381	-111		-5.9

[a]Reference 18.
[b]Reference 19.
[c]Reference 20.
[d]Reference 21.
[e]Reference 22.
[f]Reference 23.
[g]Reference 24.
[h]Reference 25.
[i]Reference 35.

$\partial E_0/\partial M_I$ are listed in Table I. The fitted value of $\partial E_0/\partial M_{\mathrm{Cu}}=-524\pm16\ \mu$eV/amu (the error bars have been estimated from the value of the TA coefficient, which was neglected when determining $\partial E_0/\partial M_{\mathrm{Cu}}$) agrees very well with the directly measured one ($-550\pm12\ \mu$eV/amu).

VI. CHALCOPYRITES

Information about the temperature dependence of the lowest gaps (usually direct and also labeled E_0) of the copper and silver chalcopyrites (I-III-VI_2 compounds) is found scattered throughout the literature, mostly limited to the 0–300-K region.[18–25] Most of these data show anomalies similar to those observed for the cuprous halides, a fact which seems to have remained unnoticed by most authors (note, however, that in Ref. 19 *ad hoc* fits with two oscillators, with contributions of opposite signs, were performed). We have listed in Table II the gaps of a number of such chalcopyrites and the change they experience from 0 to 300 K, together with the temperature T_a at which a change in the slope of $E_0(T)$ is observed. We have also included in the last column the corresponding deformation potentials $\alpha=dE_0/d\ln V$, taken from Refs. 20 and 35. For comparison we have also shown the available corresponding values for the cuprous halides, for wurtzite structure AgI (AgCl and AgBr crystallize in the rocksalt structure therefore presenting a very different behavior), and for several zinc-blende-type III-V and II-VI compounds. The trends observed for these parameters in the chalcopyrites reinforce the arguments made in this paper concerning the anomalous sign of the copper (which also applies to silver) contributions to the properties under discussion, to which we can add now the deformation potential α:

(i) The differences $E_0(300\ \mathrm{K})-E_0(0)$ reverse sign and become smaller in magnitude when going from the III-V and II-VI compounds to CuCl and CuBr.

(ii) For CuI and AgI these differences also become very small although the sign reversal does not quite take place.

(iii) The corresponding behavior for the chalcopyrites lies between that of the II-VI and the I-VII compounds.

This last statement is reinforced when following the isoelectronic series of Table III.[40]

TABLE III. Data extracted from Table II for the isoelectronic sequence GaAs-ZnSe-$CuGaSe_2$-CuBr, emphasizing the monotonic variation of E_0 (300 K)-E_0 and α along the series.

	GaAs	ZnSe	$CuGaSe_2$	CuBr
$E_0(T=0)$ (meV)	1540	2770	1720	2967
$E_0(300\ \mathrm{K})-E_0(0)$	-95	-90	-35	+32
α (eV)	-9.8	-4.9	-3.9	-0.3
T_a (K)			140	100

The near cancellation of $E_0(300\ \mathrm{K})-E_0(0)$ for CuI and its negative sign can also be followed through an isoelectronic series (see Table IV).[40]

Note that whereas in the GaAs series E_0 increases with temperature for the chalcopyrite at low temperature and decreases above T_a, for the GaSb series no increase is observed at low temperature, a fact which corresponds to the results of Fig. 3 for CuI. The values of $E_0(300\ \mathrm{K})-E_0(0)$ for the chalcopyrites lie between those of the corresponding isoelectronic I-VII and II-VI compounds; this reflects the fact that only half as much copper (or silver) is present in the chalcopyrites as in the I-VII counterparts. Similar trends to those just described also apply to the deformation potential α. Hence an anomalous, positive contribution to α must result from the presence of the noble metal.

We notice that most elements in the chalcopyrites of Table

TABLE IV. Data extracted from Table II for the isoelectronic sequence GaSb-ZnTe-$CuGaTe_2$-CuI, emphasizing the monotonic variation of E_0 (300 K)-E_0 and α along the series.

	GaSb	ZnTe	$CuGaTe_2$	CuI
$E_0(T=0)$ (meV)	813	2381	1000	3057
$E_0(300\ \mathrm{K})-E_0(0)$	-88	-111	-43	-8
α (eV)	-7.0	-5.9	-3.4	-1.1
T_a (K)				180

II have more than one stable isotope (exceptions: Al, As, and I). It would be most interesting to measure the corresponding isotope effects on the E_0 gaps of chalcopyrite samples.

VII. CONCLUSIONS

We have measured the effect of changing copper isotopes on the two-photon spectra of CuI and the temperature dependence of the lowest exciton, corresponding to the E_0 gap. For CuBr we have measured the corresponding isotope effects for both constituents. The results have been used to interpret the anomalous temperature dependence of the E_0 gaps of these materials. The behavior of $E_0(T)$ is particularly interesting for CuI where we have nearly complete cancellation of the contributions of the copper and iodine vibrations to the temperature shift of E_0. For CuBr, a reversal of the phonon eigenvectors was needed to explain the isotope effects, in agreement with results previously reported from Raman measurements.[27]

We have examined similar effects observed for the copper and silver chalcopyrites (I-III-VI_2) and pointed out that the contribution of the noble metals is also negative but less than that in the binary halides. This follows naturally from the amount of the noble metal present in these compounds.

J.S. acknowledges financial support from the Max-Planck-Gesellschaft and the Ministerio de Educación, Cultura y Deportes (Spain) through the Plan Nacional de Formación del Profesorado Universitario.

[1] M. Cardona, Phys. Rev. **129**, 69 (1963).
[2] A. Goldmann, Phys. Status Solidi B **81**, 9 (1977).
[3] K. Shindo, A. Morita, and K. Kamimura, Proc. Phys. Soc. Jpn. **20**, 2054 (1965).
[4] S. Ves, D. Glötzel, and M. Cardona, Phys. Rev. B **24**, 3073 (1981).
[5] A. Blacha, S. Ves, and M. Cardona, Phys. Rev. B **27**, 6346 (1983).
[6] K. Reimann and St. Rübenacke, Phys. Rev. B **49**, 11 021 (1994).
[7] A. Göbel, T. Ruf, M. Cardona, C. T. Lin, J. Wrzesinski, M. Steube, K. Reimann, J.-C. Merle, and M. Joucla, Phys. Rev. B **57**, 15 183 (1998).
[8] P. Etchegoin, J. Weber, M. Cardona, W. L. Hansen, K. M. Itoh, and E. E. Haller, Solid State Commun. **83**, 843 (1992).
[9] C. Parks, A. K. Ramdas, S. Rodríguez, K. M. Itoh, and E. E. Haller, Phys. Rev. B **49**, 14 244 (1994).
[10] M. Cardona, Phys. Status Solidi A **188**, 1209 (2001).
[11] L. F. Lastras-Martínez, T. Ruf, M. Konuma, M. Cardona, and D. E. Aspnes, Phys. Rev. B **61**, 12 946 (2000).
[12] A. Göbel, T. Ruf, J. M. Zhang, R. Lauck, and M. Cardona, Phys. Rev. B **59**, 2749 (1999).
[13] F. Raga, R. Kleim, A. Mysyrowicz, J. B. Grun, and S. Nikitine, J. Phys. (Paris), Colloq. **28**, C3-116 (1967).
[14] Y. Kaifu and T. Komatsu, Phys. Status Solidi B **48**, K125 (1971).
[15] V. K. Miloslavskii and O. N. Yunakova, Opt. Spektrosc. (USSR) **57**, 86 (1984) [Opt. Spectrosc. **57**, 51 (1984)].
[16] S. Lewonczuk, J. G. Gross, and J. Ringeisen, J. Phys. (France) Lett. **42**, L91 (1981).
[17] Iodine is one of the few elements with only one stable isotope, ^{127}I; hence, $\partial E_0/\partial M_I$ could not be measured.
[18] S. Chichibu, H. Nakanishi, and S. Shirakata, Appl. Phys. Lett. **66**, 3513 (1995).
[19] M. Quintero, C. Rincón, R. Tovar, and J. C. Woolley, J. Phys.: Condens. Matter **4**, 1281 (1992).
[20] S.-H. Wei, A. Zunger, I.-H. Choi, and P. Y. Yu, Phys. Rev. B **58**, R1710 (1998).
[21] A. Rivero, M. Quintero, Ch. Power, J. González, R. Tovar, and J. Ruiz, J. Electron. Mater. **26**, 1428 (1997).
[22] M. Quintero, B. D. Marks, and J. C. Woolley, J. Appl. Phys. **66**, 2402 (1989).
[23] L. Artus and Y. Bertrand, Solid State Commun. **61**, 733 (1987).
[24] V. A. Aliyev, G. D. Guseinov, F. I. Mamedov, and L. M. Chapanova, Solid State Commun. **59**, 745 (1986).
[25] M. Quintero, R. Tovar, C. Bellabarba, and J. C. Woolley, Phys. Status Solidi B **162**, 517 (1990).
[26] S. Suga, K. Cho, and M. Bettini, Phys. Rev. B **13**, 943 (1976).
[27] J. Serrano, T. Ruf, F. Widulle, C. T. Lin, and M. Cardona, Phys. Rev. B **64**, 045201 (2001).
[28] C. T. Lin, E. Schönherr, A. Schmeding, T. Ruf, A. Göbel, and M. Cardona, J. Cryst. Growth **167**, 612 (1996).
[29] C. T. Lin *et al.* (unpublished).
[30] D. Fröhlich, in *Nonlinear Spectroscopy of Solids: Advances and Applications*, edited by B. Di Bartolo and B. Bowlby (Plenum, New York, 1994), p. 289.
[31] D. Fröhlich, E. Mohler, and P. Wiesner, Phys. Rev. Lett. **26**, 554 (1971); D. Fröhlich and W. Nieswand, Philos. Mag. B **70**, 321 (1994).
[32] S. Suga, K. Cho, Y. Niji, J. C. Merle, and T. Sander, Phys. Rev. B **22**, 4931 (1980).
[33] Y. Nozue, J. Phys. Soc. Jpn. **51**, 1840 (1982).
[34] D. Karaiskaj, M. L. W. Thewalt, T. Ruf, M. Cardona, H.-J. Pohl, G. G. Deviatych, P. G. Sennikov, and H. Riemann, Phys. Rev. Lett. **86**, 6010 (2001).
[35] *Landolt-Börnstein, Numerical Data and Functional Relationships in Science and Technology*, Group III, Vol. 17, Pt. a, Vol. 22, Pt. a, and Vol. 41, Pt. b (Springer-Verlag, Berlin, Heidelberg, 1982, 1999).
[36] J. Serrano, M. Cardona, and T. Ruf, Solid State Commun. **113**, 411 (2000).
[37] M. Cardona, T. Ruf, and J. Serrano, Phys. Rev. Lett. **86**, 3923 (2001).
[38] T. Goto and T. Takahashi, J. Phys. Soc. Jpn. **24**, 314 (1968).
[39] We have taken for this calculation $\alpha = -1.2$ eV [$-1.10(7)$ from Ref. 35].
[40] Note that the kink at T_a is only observed in the compounds containing copper and silver, and the value of T_a decreases with the content of noble metal.